FDTD-Net: A Deep Learning technique to model the FDTD Method

M. A. Alvarez-Navarro, PhD(c) [1], E. Arzuaga-Cruz, PhD[2], and H. Sierra-Gil, PhD[3]
[1,2,3]University of Puerto Rico at Mayaguez, Puerto Rico, michael.alvarez2@upr.edu, emmanuel.arzuaga@upr.edu, heidy.sierra1@upr.edu

***Abstract*– The Finite-Difference Time-Domain (FDTD) method is a numerical modeling technique used by researchers as one of the most accurate methods to simulate the propagation of an electromagnetic wave through an object over time. Due to the nature of the method, FDTD can be computationally expensive when used in complex setting such as light propagation in highly heterogenous object such as the imaging process of tissues. In this paper, we explore a Deep Learning (DL) model that predicts the evolution of an electromagnetic field in a heterogeneous medium. In particular, modeling for propagation of a Gaussian beam in skin tissue layers. This is relevant for the characterization of microscopy imaging of tissues. Our proposed model named FDTD-net, is based on the U-net architecture, seems to perform the prediction of the electric field (EF) with good accuracy and faster when compared to the FDTD method. A dataset of different geometries was created to simulate the propagation of the electric field. The propagation of the electric field was initially generated using the traditional FDTD method. This data set was used for training and testing of the FDTD-net.**

The experiments show that the FDTD-net learns the physics related to the propagation of the source in the heterogeneous objects, and it can capture changes in the field due to changes in the object morphology. As a result, we present a DL model that can compute a propagated electric field in less time than the traditional method.

***Keywords*-- FDTD method, U-net model, Encoder-Decoder network, Heterogeneous medium.**

I. Introduction

Computational Electromagnetics (CEM) predicts the solution of diverse problems involving that wave propagation, light scattering, antenna performance, radar signature, and the frequency response of materials under varied conditions [1]. In optical applications, understanding light as an electromagnetic wave enables us to study light-object interactions. Therefore, the numerical analysis from electromagnetic theory can be used in the development and characterization of advanced techniques for optical imaging [2], [3]. Computational methods such as the finite-difference time-domain (FDTD) method are based on the direct solution of the wave equation. They can accurately model the light interaction with objects of arbitrary shape and structural details [4]. However, achieving high accurate simulations can be timely and computational expensive.

Parallel computing has been presented as an alternative to deal with the computational cost in the CEM techniques. For the FDTD method, parallel architectures are specialized in the spatial domain [5], and time domains [6]. The optimization consists of reorganizing the operation in subdomains. The subdomains can be resolved separately, and each solution is assembled with the primary domain after determining the subdomains. The assembly requires additional postprocessing in the boundaries of each subdomain because these parallel strategies can cause a loss in the accuracy of the solution.

Artificial intelligence models have been presented for CEM while reducing the execution time and computational iterations. Qi et. al. [7] proposed an implementation of the U-net to model the electric field predicted by the finite-difference frequency-domain (FDFD) method for homogeneous mediums that contain two refractive indexes and regular shapes with reasonable accuracy. Methodologies that include combining the FDTD method with neural network architectures [8]–[10] have also been proposed. Yao and Jiang proposed a Recurrent Neural Network FDTD (RNN-FDTD) model and a Convolution Neural Network FDTD (CNN-FDTD) model [8] to compute the electric field and the absorption at the boundary as a general solution for the wave equation. These neural network architectures aim to reduce the number of iterations that are required by the FDTD method to achieve high accuracy. The resulting models have the advantage of reducing the prediction time. However, the precision is lower compared to the deterministic techniques.

Yao and Jiang have also proposed strategies to replace the absorption boundary condition from the traditional perfectly matched layer (PML) with a fully connected network [9] and a long short-term memory (LTSM) model [10]. The goal is to provide a way to reduce the simulated thickness to one cell in the boundary domain. The implementation of these strategies is computationally complex, and the performance of the neural networks is comparable to the traditional approach. However, more training samples are required when compared to other methods based on deep neural models.

This paper presents a deep learning model based on an Encoder-Decoder network called FDTD-net. The proposed FDTD-net aims to model the electric field that results by propagating a Gaussian source through a highly heterogeneous object. To the best of our knowledge, there is no computational framework with these characteristics. The FDTD-net is trained with a dataset composed of the electric fields generated by the traditional FDTD method. The electric field is propagated in an object with heterogeneous geometries. The results show that the proposed model can achieve an acceptable accuracy in predicting the electric field propagated in the mediums while reducing the prediction time. This article is organized as follows: a description of the geometry's dataset, a brief

Digital Object Identifier: (only for full papers, inserted by LACCEI).
ISSN, ISBN: (to be inserted by LACCEI).
DO NOT REMOVE

description of the FDTD method, a description of the proposed FDTD-net, a results section, and the conclusions section.

II. Methodology

A. Object's geometry

The object is simulated in terms of index refraction (n). The geometries are inspired in a representation of the human skin layers presented in [11]. A two-dimensional matrix represents the object's geometry. The rows and columns represent the spatial dimensions. In the matrix, the value of each pixel represents the electromagnetic properties: permeability and relative permittivity of the material, where the values define the refractive index of the electromagnetic radiation. The refractive index of electromagnetic radiation is: $n = \sqrt{\varepsilon_r \mu_r}$ where ε_r is the material's relative permittivity, and μ_r is the relative permeability.

We create square matrices of 256 pixels, equivalent to 10.54 [μm]. The geometries simulate the skin's dermis with layers of cells and their components, such as the nucleus, cytoplasm, mitochondria, and melanin. The cells are randomly generated by variations in the elliptical form, position, and separation of the cells. Figure 2 first column presents four random simulated geometries. Each geometry contains water (n=1.33), sinusoidal junction (n=1.37), dermis (n=1.40), cells with nucleus (n=1.39), cytoplasm (n=1.37), and intercellular fluid (n=1.34), mitochondria (n=1.42); and melanin (n=1.7). A total of 1232 samples with at least 3 different refractive indices were generated.

B. FDTD Method

The Finite-Difference Time-Domain (FDTD) method is a deterministic method developed by Yee in 1966 [12] that consists of solving the differential form of Maxwell's equations:

$$\nabla \times H = \frac{\partial D}{\partial t} + J\,, \tag{1}$$

$$-\nabla \times E = \frac{\partial B}{\partial t}\,, \tag{2}$$

where H is the magnetic field vector, D is the electric displacement vector, J is the electric current density vector, E is the electric field vector, B is the magnetic flux density vector.

The matrix form of the FDTD method for 2 dimensions and transverse magnetic mode [13] corresponds to:

$$\mathcal{E}_z^n = C_\mathcal{E}\mathcal{E}_z^{n-1} + C_{h_y}\,\Delta_x\mathcal{H}_y^n + C_{h_x}\,\Delta_y\mathcal{H}_x^n\,, \tag{3}$$

$$\mathcal{H}_x^n = C_{\mathcal{H}_x}\mathcal{H}_x^{n-1} + C_{hxz}\,\Delta_y\mathcal{E}_z^n\,, \tag{4}$$

$$\mathcal{H}_y^n = C_{\mathcal{H}_y}\mathcal{H}_z^{n-1} + C_{hyz}\,\Delta_x\mathcal{E}_z^n\,, \tag{5}$$

where the constants are:

$$C_\mathcal{E} = \frac{2\epsilon - \Delta t\sigma}{2\epsilon + \Delta t\sigma}\,, \tag{6}$$

$$C_{h_y} = \frac{2\Delta t}{(2\epsilon + \Delta t\sigma)\Delta x}\,, \tag{7}$$

$$C_{h_x} = \frac{-2\Delta t}{(2\epsilon + \Delta t\sigma)\Delta y}\,, \tag{8}$$

$$C_{\mathcal{H}_x} = \frac{2\mu - \Delta t\sigma}{(2\mu + \Delta t\sigma)\Delta y}\,, \tag{9}$$

$$C_{hxz} = \frac{-2\Delta t}{(2\mu + \Delta t\sigma)\Delta y}\,, \tag{10}$$

$$C_{\mathcal{H}_y} = \frac{2\mu - \Delta t\sigma}{(2\mu + \Delta t\sigma)\Delta x}\,, \tag{11}$$

$$C_{hyz} = \frac{2\Delta t}{(2\mu + \Delta t\sigma)\Delta x}\,, \tag{12}$$

and the differential matrices are:

$$\Delta_x\mathcal{H}_y^n = \mathcal{H}_y^n(i,j) - \mathcal{H}_y^n(i-1,j)\,, \tag{13}$$

$$\Delta_y\mathcal{H}_x^n = \mathcal{H}_x^n(i,j) - \mathcal{H}_x^n(i,j-1)\,, \tag{14}$$

$$\Delta_y\mathcal{E}_z^n = \mathcal{E}_z^n(i,j+1) - \mathcal{E}_z^n(i,j)\,, \tag{15}$$

$$\Delta_x\mathcal{E}_z^n = \mathcal{E}_z^n(i+1,j) - \mathcal{E}_z^n(i,j)\,. \tag{16}$$

Inside the propagation medium, we set the conductivity equal to zero because there aren't internal electric and magnetic sources. On the computational boundaries, we are set to a fictitious conductivity following the perfectly matched layer (PML) [14]. The stability of the FDTD method depends on the Courant-Friedrichs-Lewy (CFL) condition and the spatial discretization restricted by wavelength condition [15]. From the CFL condition, the time step must satisfy:

$$\Delta t \leq \frac{\Delta}{\sqrt{2}\,(c_0/n_{min})}\,, \tag{17}$$

where Δt is the temporal step size; Δ is the spatial step size; $\sqrt{2}$ correspond to the 2-dimensional problem; c_0 is the speed of light in free space; and n_{min} is the minimum index of refraction in the propagation medium. For the spatial discretization the condition is: $\Delta \leq \frac{\lambda}{n_{max}}$ where n_{max} is the maximum index of refraction in the propagation medium. The experiment propagates a sinusoidal electric voltage source in the z-direction for all mediums described in Section II-A. The source term is formulated as the real part of the complex electric field E_z propagated by a Gaussian wave [11]:

$$E_z(x,y_0) = f_{ert}(t)\exp(i\omega t)\exp\left(-\left[\frac{x-(X_{max}/4)}{2X_{max}/6}\right]^2\right) exp\left(i\left[f_l^2 + \left(x - \tfrac{X_{max}}{2}\right)^2\right]^{1/2} - f_l\right). \tag{18}$$

C. FDTD-net model

In this paper, a deep learning model is employed to approximate the solution of Maxwell's equations given by the iterative process of the FDTD method in the form of system (3)-(5). The model requires two input matrices to perform the prediction of the propagated electromagnetic field. The input matrices are the concatenation of a discrete representation of the medium and the electromagnetic source. The refractive index describes the medium, and the source corresponds to the electromagnetic field generated by a Gaussian beam source in the vacuum. The model's output represents the modulated source by the interaction of the source with the medium.

To achieve electromagnetic field predictions by the image generation process, we use the Encoder-Decoder architecture in a similar configuration to the U-net model [16]. A U-net is a network that is commonly for image segmentation and contains residual blocks configuration to ease the training of networks by adding shortcut connections between the weight layers.

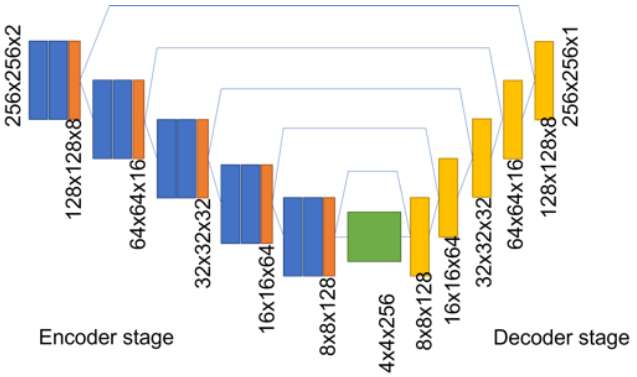

Fig. 1. FDTD-net architecture to model the FDTD method.

The proposed FDTD-net model has an asymmetrical configuration characterized by a modified version of the residual blocks [17]. The residual blocks are used to create convolutional and transpose-convolutional blocks. The encoder stage is formed by a sequence of five levels of two convolutional blocks (blue rectangle) and a Pooling layer (orange rectangle). The decoder stage is formed by a succession of five levels of transpose-convolution blocks. Figure 1 shows the encoder and decoder stages of the proposed FDTD-net model.

The convolutional block is defined by a modified residual block composed of the addition between a Conv. layer and a sequence of Conv-CReLU-Conv-Gated layers. The Pooling layer is used to reduce the spatial dimension of the input data from 256 x 256 to 8 x 8 pixels; in each level, the spatial dimension is comprised by a factor of 2. The transpose-convolution block is defined by a modified residual block composed of the addition between a TrConv. layer and a sequence of TrConv-CReLU-TrConv-Gated layers. Each encoder unit has connected with the decoder unit of the same spatial size. There is a convolutional sequence between the encoder-decoder stages to maximize the flux information.

D. Training model

For the input of the FDTD-net model, we concatenate the geometry and the electric field propagated in the vacuum. The correspondent target is the electric source propagated by the FDTD method in the input geometry. The training and testing samples are split into 80 and 20 percent, respectively.

In terms of parameters, each convolution layer has a variable number of filters with a fixed size; for example, the first convolutional block has a weight matrix of 3x3x2x8 and a bias matrix of 1x1x8, so there are 144 and 8 parameters to train in the initial convolutional layer. In total, the FDTD-net model have 5'099,421 learnable parameters.

The FDTD-net model and the FDTD method were implemented using MATLAB® (2020b - Academic license) programming language. We did all experiments in a Windows 10 Education Desktop computer, using an Intel(R) Core(TM) i7-8700 CPU 3.20 (GHz) with 16 GB RAM, in the Laboratory for Applied Remote Sensing and Image Processing (LARSIP) at the University of Puerto Rico, Mayaguez Campus.

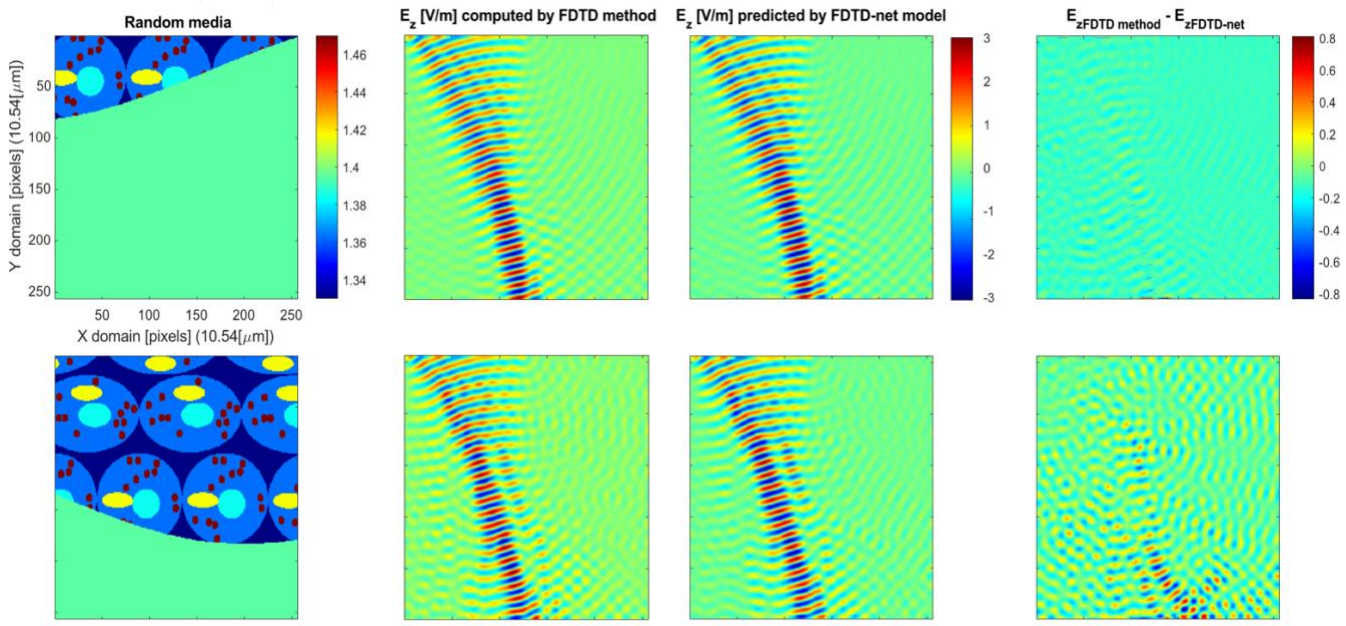

Fig. 2. Example of two random medium of simulation (first column), Electric field propagated by FDTD method (second column), Electric field estimate by FDTD-net model (third column), and the difference between the Electric fields computed by the FDTD method and the FDTD-net model (last column). The refractive index describes the properties of the heterogeneous material. The spatial size of 256x256 pixels of simulation correspond to a square of 10.54 [μm] by side. The medium is a model of tissue with cells of different size and components.

III. Results

This section presents the results of the trained FDTD-net to model the FDTD method for heterogeneous mediums. In Figure 2, the first column corresponds to the propagation medium, the second column is the electric field propagated by the FDTD method, the third column is the electric field predicted by the FDTD-net, and the fourth column shows the difference between the electric fields computed by the two methods. Each row in Figure 2 shows corresponds to an object randomly selected. We also compute the structural similarity index metric (SSIM) [18] for each pair of the electric fields. To calculate SSIM, we represent each matrix as an image of 8-bit. For the objects presented in Figure 2, the SSIM values are: [**0.8448**, **0.4674**] for rows one and two, respectively. For the testing samples, FDTD-net obtain a mean value of the SSIM of **0.8082**. Table 1 shows the execution times for the training and testing stages of the FDTD-net model and the execution times of the FDTD method.

TABLE I
TIME EXECUTION PERFORMANCE

FDTD-net time	
1) Training time	235.53 (min)
2) Testing time	
a. Load net	0.5816 (s)
b. Predict one media	0.0074 (s)
c. Predict all media	9.1612 (s)
FDTD method	
Compute one media	17.9385 (s)
Compute all media	368.33 (min)

IV. Conclusions and Future work

This article presents an FDTD-net model for calculating the propagated electric field across a non-homogeneous object. The results show that FDTD-net can follow the changes in the electric field in terms of the heterogeneities of the medium. This approach provides a good performance based on the metrics values and exploits the advantage of the DL models in time execution. As shown in Table 1, the FDTD-net model is 30 times faster than the FDTD method in predicting one media. The network loading time is approximately half-second. The execution time to predict the field for all the testing samples is ˜2400 times faster than the FDTD method.

Future work includes exploring modification of the FDTD-net by augmenting the number of layers to increase the prediction accuracy. A modified model version is being studied by tuning the parameters to perform a more precise prediction of the electric field.

Acknowledgment

We thank Mr. Carlos A. Theran Suarez for his participation in the discussion about the selection of the Deep Learning networks. This work is partially supported by NSF Grant No. OAC-1750970 and NSF Award No. OIA-1849243.

References

[1] P. Sumithra and D. Thiripurasundari, "A review on computational electromagnetics methods," *Adv. Electromagn.*, vol. 6, no. 1, pp. 42–55, 2017, doi: 10.7716/aem.v6i1.407.

[2] A. Canales-Benavides *et al.*, "Accessible quantitative phase imaging in confocal microscopy with sinusoidal-phase synthetic optical holography," *arXiv*, 2019, doi: 10.1364/ao.58.000a55.

[3] K. De Haan, Y. Rivenson, Y. Wu, and A. Ozcan, "Deep-Learning-Based Image Reconstruction and Enhancement in Optical Microscopy," *Proc. IEEE*, vol. 108, no. 1, pp. 30–50, 2020, doi: 10.1109/JPROC.2019.2949575.

[4] M. Schnell, S. Gupta, T. P. Wrobel, M. G. Drage, R. Bhargava, and P. S. Carney, "High-resolution label-free imaging of tissue morphology with confocal phase microscopy," *arXiv*. Optica, Sep. 04, 2020. doi: 10.1364/optica.395363.

[5] J. L. Volakis, D. B. Davidson, C. Guiffaut, and K. Mahdjoubi, "A parallel FDTD algorithm using the MPI library," *IEEE Antennas Propag. Mag.*, vol. 43, no. 2, pp. 94–103, 2001, doi: 10.1109/74.924608.

[6] S. Ohnuki, R. Ohnishi, D. Wu, and T. Yamaguchi, "Time-Division Parallel FDTD Algorithm," *IEEE Photonics Technol. Lett.*, vol. 30, no. 24, pp. 2143–2146, 2018, doi: 10.1109/LPT.2018.2879365.

[7] S. Qi, Y. Wang, Y. Li, X. Wu, Q. Ren, and Y. Ren, "Two-Dimensional Electromagnetic Solver Based on Deep Learning Technique," *IEEE J. Multiscale Multiphysics Comput. Tech.*, vol. 5, pp. 83–88, 2020, doi: 10.1109/JMMCT.2020.2995811.

[8] H. M. Yao and L. J. Jiang, "Machine Learning Based Neural Network Solving Methods for the FDTD Method," *2018 IEEE Antennas Propag. Soc. Int. Symp. Usn. Natl. Radio Sci. Meet. APSURSI 2018 - Proc.*, no. 5, pp. 2321–2322, 2018, doi: 10.1109/APUSNCURSINRSM.2018.8608745.

[9] H. M. Yao and L. Jiang, "Machine-Learning-Based PML for the FDTD Method," *IEEE Antennas Wirel. Propag. Lett.*, vol. 18, no. 1, pp. 192–196, Jan. 2019, doi: 10.1109/LAWP.2018.2885570.

[10] H. M. Yao and L. Jiang, "Enhanced PML Based on the Long Short Term Memory Network for the FDTD Method," *IEEE Access*, vol. 8, pp. 21028–21035, 2020, doi: 10.1109/ACCESS.2020.2969569.

[11] B. Simon and C. A. DiMarzio, "Simulation of a theta line-scanning confocal microscope," *J. Biomed. Opt.*, vol. 12, no. 6, p. 064020, 2007, doi: 10.1117/1.2821425.

[12] Kane Yee, "Numerical solution of initial boundary value problems involving maxwell's equations in isotropic media," *IEEE Trans. Antennas Propag.*, vol. 14, no. 3, pp. 302–307, May 1966, doi: 10.1109/TAP.1966.1138693.

[13] V. Elsherbeni, Atef Z and Demir, The finite-difference time-domain method for electromagnetics with MATLAB simulations. 2016.

[14] B. Jean-Pierre and Bringer, J.-P., "A Perfectly Matched Layer for the Absorption of Electromagnetic Waves," *J. Comput. Phys.*, vol. 114, no. 2, pp. 185–200, 1994, doi: 10.1006/jcph.1994.1159.

[15] A. Taflove and M. E. Brodwin, "Numerical Solution of Steady-State Electromagnetic Scattering Problems Using the Time-Dependent Maxwell's Equations," *IEEE Trans. Microw. Theory Tech.*, vol. 23, no. 8, pp. 623–630, 1975, doi: 10.1109/TMTT.1975.1128640.

[16] O. Ronneberger, P. Fischer, and T. Brox, "U-net: Convolutional networks for biomedical image segmentation," in Lecture Notes in Computer Science (including subseries Lecture Notes in Artificial Intelligence and Lecture Notes in Bioinformatics), 2015, vol. 9351, pp. 234–241. doi: 10.1007/978-3-319-24574-4_28.

[17] K. He, X. Zhang, S. Ren, and J. Sun, "Deep Residual Learning for Image Recognition," in *2016 IEEE Conference on Computer Vision and Pattern Recognition (CVPR)*, Jun. 2016, vol. 2016-Decem, no. 8, pp. 770–778. doi: 10.1109/CVPR.2016.90.

[18] Z. Wang, A. C. Bovik, H. R. Sheikh, and E. P. Simoncelli, "Image quality assessment: From error visibility to structural similarity," *IEEE Trans. Image Process.*, vol. 13, no. 4, pp. 600–612, 2004, doi: 10.1109/TIP.2003.819861.